J Nondestruct Eval (2011) 30:201–212
DOI 10.1007/s10921-011-0108-6

Photogrammetry Assisted Measurement of Interstory Drift for Rapid Post-disaster Building Damage Reconnaissance

Fei Dai · Suyang Dong · Vineet R. Kamat · Ming Lu

Received: 27 October 2010 / Accepted: 14 June 2011 / Published online: 30 June 2011

Abstract Timely and accurate evaluation of damage sustained by buildings after seismic events such as earthquakes or blasts is critical to determine the buildings' safety and suitability for their future occupancy. Time used in conducting the evaluations substantially affects the duration for which the potentially damaged buildings remain unusable. The elapsed time may lead to direct economic losses to both public and private owners, and society at large. The presented research investigates the application of close-range photogrammetry surveying techniques and Augmented Reality (AR) visualization to design a semi-automated method for rapidly measuring structural damage induced in tall buildings by seismic events such as earthquakes or explosions. Close-range photogrammetry algorithms were designed to extract spatial information from photographic image data, and geometrically measure the horizontal drift (also called interstory drift) sustained at key floors along the edge of a damaged building. The measured drift can then be used to compute damage indices that correlate the drift to the building's structural integrity and safety. In this research, the measurement accuracy of the calculated drift using photogrammetry principles is particularly studied. The experimental results achieved an acceptable and usable accuracy level of 5 mm using a consumer grade digital SLR camera, demonstrating the potential of photogrammetry assisted rapid measurement of earthquake-induced building damage. It is expected that in the future, as advances in optical-sensing and positioning technologies continue to make high-end cameras and measurement systems (GPS, compass) more affordable, higher accuracy will be practically achievable for further improvement in measurements using the proposed method.

Keywords Building · Damage · Earthquakes · Photogrammetry · Computer applications · Graphic methods · Reconnaissance

1 Introduction

Timely and accurate evaluation of damage sustained by buildings after seismic events such as earthquakes or blasts is critical to determine the buildings' safety and suitability for their future occupancy. Time used in conducting the evaluations substantially affects the duration for which the potentially damaged buildings remain unusable. The elapsed time may lead to direct economic losses to both public and private owners, and society at large. Current practice of evaluating damage to buildings mainly resorts to licensed inspectors manually inspecting the building's integrity and habitability based on their personal experience and knowledge. Though inspection guidelines exist (for example, in ATC-20 [1] and ATC-20-2 [2]), the work of manual inspection remains labor-intensive and time-consuming, and the results are subjective and can often be error-prone [3].

Fei Dai is S.M.ASCE.
Vineet R. Kamat is M.ASCE.
Ming Lu is M.ASCE.

F. Dai · S. Dong · V.R. Kamat (✉)
Dept. of Civil & Environmental Engineering, Univ. of Michigan, 2340 G.G. Brown, 2350 Hayward, Ann Arbor, MI 48109, USA
e-mail: vkamat@umich.edu

F. Dai
e-mail: cefdai@gmail.com

S. Dong
e-mail: dsuyang@umich.edu

M. Lu
Dept. of Civil & Environmental Engineering, Univ. of Alberta, Edmonton, Alberta T6G 2W2, Canada
e-mail: mlu6@ualberta.ca

Quantitative measurement of damage is an effective means that provides a basis for more reliable estimation of building safety. The interstory drift, defined as the relative translational displacement between consecutive floors, is an important engineering demand parameter that represents the allowable deformation level in a structure. One method of estimating interstory drift is by using acceleration data obtained from structural health monitoring sensors preinstalled in a structure [7]. However, this method requires multiple sensors deployed on building floors and substantial signal processing which is still unreliable [7]. Moreover, deploying an elaborate scheme of sensors in existing buildings on a large scale is expensive from a retrofit perspective since most of the nation's buildings were constructed about 50 years ago. Non-contact evaluation methods are thus clearly a viable alternative.

Non-contact remote sensing technologies entail the application of various spacecraft or aircraft platforms to capture remotely sensed imageries by using synthetic aperture radars or optical imaging devices. The acquired images are either compared with previous images of the same area [4] or analyzed by specific computer vision algorithms such as the watershed segmentation [5] to detect any changes on a building that might have occurred as post-earthquake damage. Although remote sensing techniques are valuable in estimating hazard patterns for large areas, quantitative assessment of damage about a particular building is difficult to achieve by this technique with an adequate level of accuracy, due to (1) limited resolution of the satellite or aerial images, for instance, the reported highest resolution of the commercial satellite images available is only 0.41 m [6], and (2) fixed pose of the imaging device applied, preventing sufficient features of the damaged building elements to be revealed.

The presented research makes an attempt to design an accurate yet simplistic approach to rapidly measure the structural damage induced in tall buildings by seismic events such as earthquakes or explosions by investigating the application of close-range photogrammetry surveying techniques and Augmented Reality (AR) visualization. Close-range photogrammetry algorithms are designed to extract spatial information from photographic image data, and geometrically measure the horizontal drift (interstory drift) sustained at key floors along the edge of a damaged building. The measured drift can then be used to compute damage indices that correlate the drift to the building's structural integrity and safety.

In this research, vision-based AR techniques identify the pixel positions of key points along a building's edge in photographs taken with consumer grade digital SLR cameras, and close-range photogrammetry computes the 3D coordinates of those points into the global object space, considering only the drift component that is perpendicular to the direction of the camera's line of sight. The interstory drift can be subsequently derived by comparing the shifted position of each floor against the pre-disaster outer geometry of the inspected building that is obtained or available a-priori from building owners or government databases. The Global Positioning System (GPS) and 3D electronic compasses are used to track the position and orientation of the camera's perspective.

Studying the measurement accuracy of the calculated drift using photogrammetry has been a primary focus of this research. Theoretically, components that account for measurement error mainly comprise the internal errors induced by the camera lens distortion, calculated approximation of the principal distance, the combination of the camera resolution, shooting distance and the focal length, and the external errors transferred from the tracking systems utilized to obtain the camera position and angular orientation. This research models the internal errors as mathematical formulations and correspondingly proposes solutions to minimize those errors. In order to quantitatively assess the level of accuracy, three groups of laboratory experiments were conducted to simulate a building damaged in an earthquake. A two-story reconfigurable steel frame was designed to physically simulate a building structure. The frame was calibrated with known displacement value at the second floor, and images were taken with a Canon EOS Rebel T1i digital camera. The images were post-processed to yield the spatial coordinates of two bolted connections on each of the frame's two floors. By subtracting horizontal axis components of the two connections, the interstory drift was computed. The experimental results revealed an accuracy level of 5 mm, demonstrating the potential of photogrammetry assisted rapid measurement of earthquake-induced building damage.

It must be noted that this research does not attempt to match or improve the general measurement accuracy that state-of-the-art commercial or high-end photogrammetry equipment can achieve in surveying applications. Rather, this paper focuses on the development of a method that utilizes consumer grade digital SLR cameras and photogrammetry concepts to rapidly measure the interstory drift of damaged building in an approximate but effective way for the purpose of reducing the time in post disaster building damage reconnaissance. Improved measurement accuracy is achievable with high-end surveying grade equipment, but the involved trade-offs conflict with this work's primary motivation. High-end photogrammetry equipment costs orders of magnitude more than consumer grade digital SLR cameras, and also requires an elaborate set-up before measurements can be made. The proposed approach capitalizes on photogrammetry concepts but uses "regular" photo cameras that can be readily deployed and used on a large scale without the need for special set-up. In addition, as advances

Fig. 1 Overview of augmented reality based reconnaissance methodology

in optical-sensing and positioning technologies continue to make superior consumer grade cameras and measurement systems (GPS, compass) more affordable, higher accuracy comparable to that obtained by surveying grade equipment will be practically achievable using the proposed method.

The remainder of this paper describes the photogrammetry assisted methodology in detail, followed by the analytical study of the internal components of cameras that induce the measurement errors, based on which the solution to minimize those errors is proposed. Finally, the laboratory experiments conducted to validate the level of measurement accuracy by photogrammetry are described, followed by a description of ongoing work towards full automation of the proposed method.

2 Methodology for Rapidly Measuring Building Damage Induced by Earthquakes

2.1 Previous Work

This study builds on prior research conducted at the University of Michigan (UM). Previous research [3] established a schematic overview of a rapid, augmented reality based, post-earthquake building damage reconnaissance method. As shown in Fig. 1, the previously studied reconnaissance methodology utilized augmented reality visualization techniques to superimpose the building's pre-earthquake geometric outer lines onto the view of the actual structure captured in real time through a video camera in an AR setting. The methodology proposed that equipped with a GPS receiver and 3D electronic compasses to track the position and orientation of the observer's perspective, the in-situ reconnaissance inspectors see through a head-mounted display to qualitatively evaluate the damage by comparing two views of the structure in a real time.

Some proof-of-concept experiments were conducted to achieve a quantitative result in the previous research. In the UM Structural Engineering Laboratory, the large-scale shear walls were selected as the test-bed and the CAD images of the walls were overlaid onto the actual wall specimens. As the cyclic loading was applied on the wall specimens, the displaced horizontal drifts were measured by placing the baselines of the CAD images in the augmented space and comparing the baselines with the edges of the actual wall specimens. The experimentally measured drifts were compared with the actual wall drifts quantified in a predetermined displacement regime. The results indicated a promising potential of applying AR for rapid building damage detection [3].

Though AR visualization techniques work well in laboratory environments, some hurdles must be addressed before AR can be implemented in a field-deployable system, one of which is that the line of sight of the inspector (video camera) must be exactly orthogonal to the floors of the inspected building such that the trigonometry calculation can be applied to infer the deformed drifts (Fig. 2a). Any oblique, even slightly, line of sight to the floors of the inspected structure will lead to non-linear, biased drifts that fail to represent the actual drift measurements (Fig. 2b). Successfully applying AR techniques to measure the building damage largely depends on the standing point and viewing perspective from where the inspector observes the structure. However, in potentially chaotic disaster scenarios, the inspectors who wear the reconnaissance systems can, at best, find it challenging

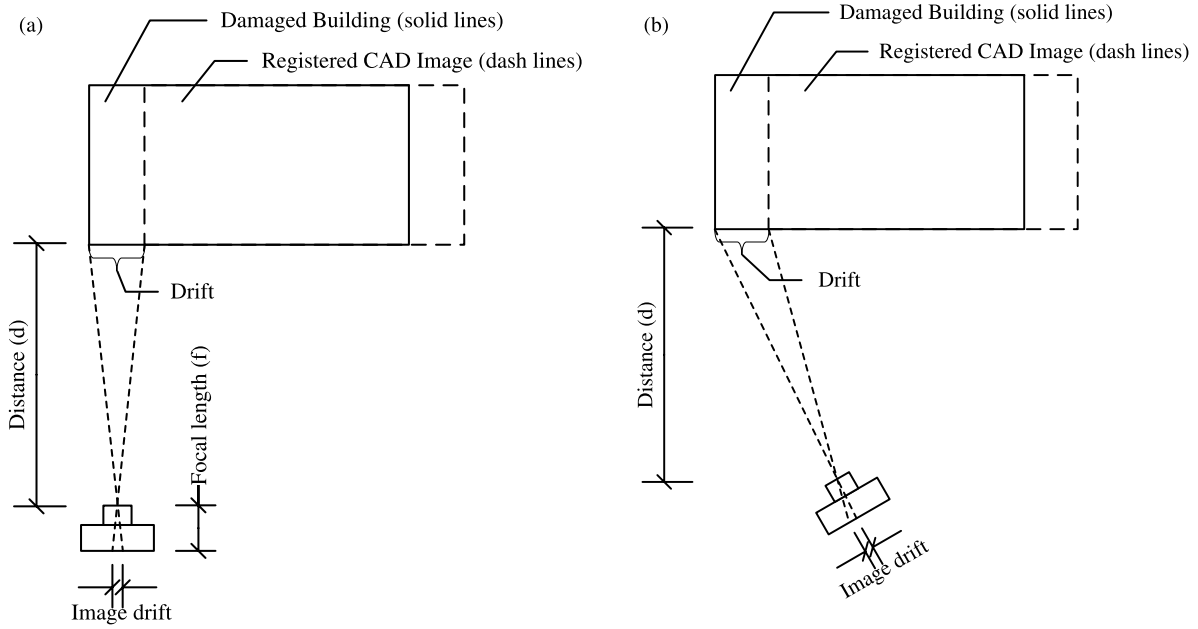

Fig. 2 Camera line of sight (**a**) orthogonal to building wall to derive the damage drift, but (**b**) oblique resulting in a non-linear, biased drift

to intuitively fine-tune their perspective to achieve the desired perpendicularity, thereby limiting the widespread use of AR visualization technology for post-earthquake reconnaissance.

Several techniques have been considered as candidates to complement AR for the ubiquitous measurement of drift induced in damaged buildings. High-precision robotic total stations survey structures with a surveying error of 2–3 mm (standard deviation). As the distances, and the horizontal and vertical angles between target points and total station itself are measured, drift of two stories can be subsequently derived. However, such equipment has the limitation of not being portable. Its weight constrains the possibility of moving such equipment from building to building quickly during the aftermath of an earthquake, and is not well suited for integration with a wearable and mobile AR inspection system. Laser scanners offer another option to perform the desired survey by mapping the depth of structures. However, the equipment used faces the same constraints described above. Typically, at least two crews are required to handle the laser scanner in doing the surveying. Alternatively, range imaging time-of-flight cameras are capable of not only capturing images of a structure, but also recoding range information of each pixel point. Examples of some advanced time-of-flight cameras available currently are MESA Imaging SR4000 [24] and PMD CamCube 3.0 [25]. The former only works indoors because of strong illumination of sunlight whereas the latter has been reported to have a working range limited to 10 m, limiting their application in the outdoor environment for rapid post-disaster building damage reconnaissance.

The surveying technique of close-range photogrammetry is powered with capacity of spatialized computation and is capable of establishing a relationship between two-dimensional (2D) photo images and the three-dimensional (3D) object space [9]. Using photogrammetry can allow inspectors to observe the structure at a standing point and viewing perspective that does not impose orthogonality, thereby complementing AR well in manipulating image data into 3D coordinates and extrapolating the interstory drifts. In the next section, the close-range photogrammetry technique is investigated to design a practical and universal method for rapid post-earthquake building damage reconnaissance.

2.2 Photogrammetry Assisted Damage Measurement

Figure 3 depicts the basic workflow of the photogrammetry assisted AR-based solution in quantifying the spatial coordinates of each floor of the damaged building. The vision-based AR technology is used to identify and extract x, y positions of building floors on the captured images. Then the x, y position data together with the geometric information of the inspected building is used as the input for post processing of the photogrammetry to derive the corresponding spatial coordinates X, Y, and Z readily for the computation of the interstory drifts sustained at key floors along the edge of a damaged building.

In the earthquake engineering community, based on the seismic design specifications such as FEMA [10], the interstory drift is used to compute indices that are unanimously suggested as a reasonable measure to reflect the extent of earthquake induced building damage. The interstory drift

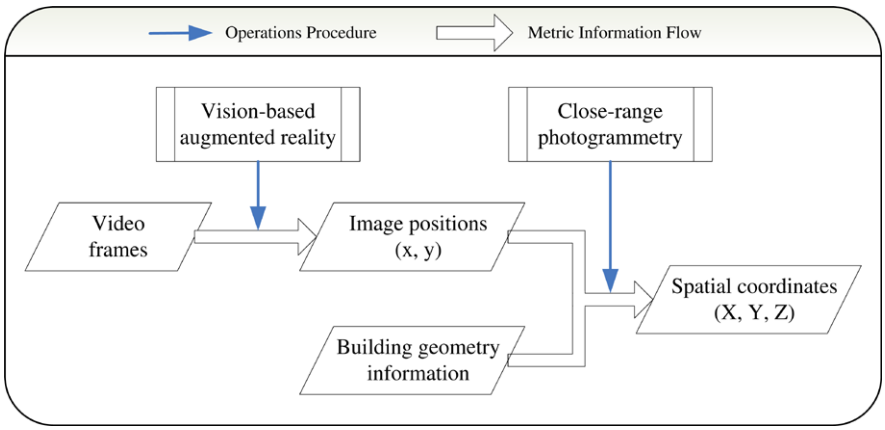

Fig. 3 Basic workflow of photogrammetry assisted post-earthquake reconnaissance

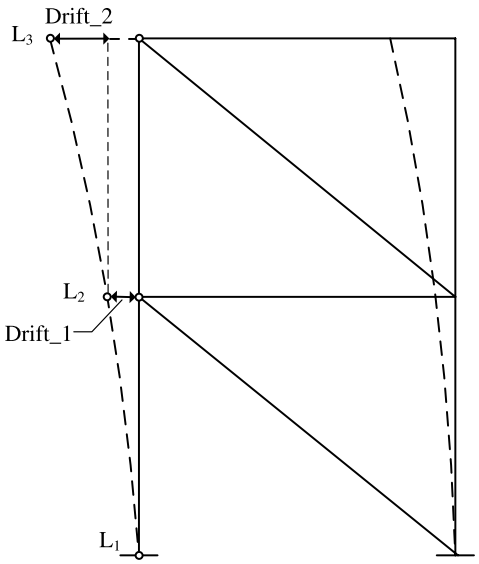

Fig. 4 A simple two-story building frame illustrating interstory drifts

can be interpreted as the horizontal displacement of each building floor that is permanently moved relative to the one beneath in regard to the damaged building. Figure 4 illustrates the interstory drifts using a simplified two-storey building frame. In Fig. 4, the building frame drawn by solid lines denotes the geometric building profile pre earthquake and the one drawn by dash curves represents the building's inclined outer walls post earthquake. From Fig. 4, the interstory drift of the first storey is the horizontal movement of the second floor (L_2) relative to the ground floor (L_1) which is denoted by Drift_1 (Fig. 4), and the interstory drift of the second storey (Drift_2 in Fig. 4) is that of the third floor (L_3) relative to the second floor (L_2) instead of the ground floor.

The two-story reconfigurable building frame constructed by the authors, and described earlier, will be used to demonstrate the computing algorithm for the interstory drift for each of the building floors, in which the 3D coordinates of the inspected floors of the damaged building should be derived first. Figure 5 models an inspector inspecting the damaged building, focusing on one of the key floors at a certain moment (e.g., the second floor).

The inspector is simply modeled by a video camera that is mounted on the inspector's helmet to capture the images of the structural damage sustained by the building. The video camera and the inspector have the same position and orientation when the building is viewed. A line of sight of the video camera is formed to link the point of the floor intersecting the building edge (e.g., L_2) in the global space with its corresponding projection on the captured image inside the camera. We denote the floor along the building edge (e.g., L_2) as its 3D coordinates in the object coordinate system of the global space (X_n, Y_n, Z_n) and its 2D coordinates on the image plane inside the camera (x_n, y_n). Thus, the line of sight can be modeled by the photogrammetric *collinearity equations* [11–13], as in (1):

$$\begin{aligned} x_n - x_p &= -c\frac{m_{11}(X_n - X_c) + m_{12}(Y_n - Y_c) + m_{13}(Z_n - Z_c)}{m_{31}(X_n - X_c) + m_{32}(Y_n - Y_c) + m_{33}(Z_n - Z_c)} \\ y_n - y_p &= -c\frac{m_{21}(X_n - X_c) + m_{22}(Y_n - Y_c) + m_{23}(Z_n - Z_c)}{m_{31}(X_n - X_c) + m_{32}(Y_n - Y_c) + m_{33}(Z_n - Z_c)} \end{aligned} \tag{1}$$

In (1), (x_p, y_p) is the *principal point* on the image plane and c is the *principal distance*. They describe the internal orientation of the camera station, which can be referred to as the projected position of the light ray on the image plane through center of the lens opening of the camera (perspective center) from infinity (*principal point*), and the perpendicular distance between the perspective center and the image plane (*principal distance*). The camera internal components can be determined by performing the camera calibration, which will be described in the ensuing section entitled "Camera Calibration". Equation (1) also has (X_c, Y_c, Z_c) and $m_{ij}(i, j = 1, 2, 3)$ to define the exterior orientation of

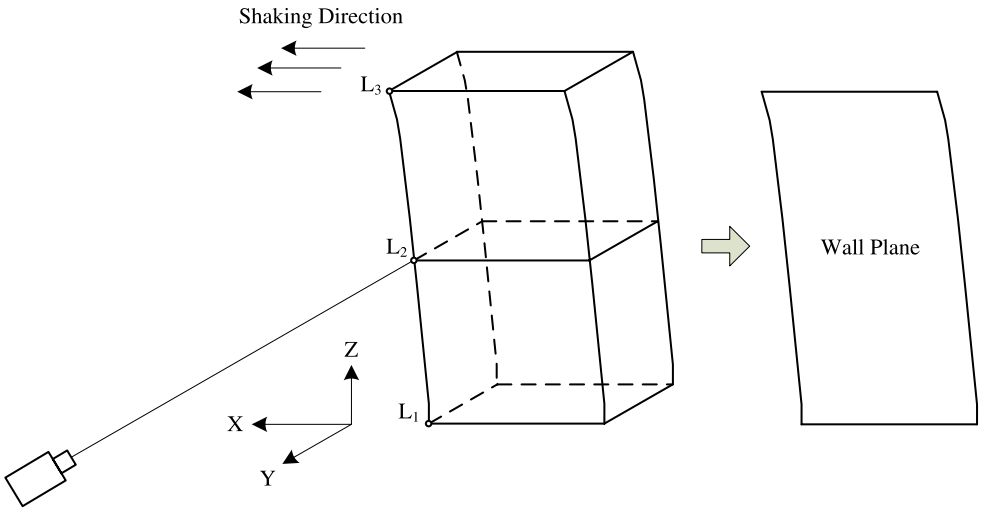

Fig. 5 An inspector inspecting the damaged building, focusing on one of the key floors (e.g., the second floor)

the camera station. (X_c, Y_c, Z_c) refer to the position of the perspective center and m_{ij} are the elements of an rotation matrix M, which are expressed as functions of the Euler orientation angles—azimuth (α), tilt (t), and swing (s) [12], as elaborated in (2):

$$\begin{aligned}
m_{11} &= -\cos\alpha\cos s - \sin\alpha\cos t\sin s \\
m_{12} &= \sin\alpha\cos s - \cos\alpha\cos t\sin s \\
m_{13} &= -\sin t\sin s \\
m_{21} &= \cos\alpha\sin s - \sin\alpha\cos t\cos s \\
m_{22} &= -\sin\alpha\sin s - \cos\alpha\cos t\cos s \\
m_{23} &= -\sin t\cos s \\
m_{31} &= -\sin\alpha\sin t \\
m_{32} &= -\cos\alpha\sin t \\
m_{33} &= \cos t
\end{aligned} \tag{2}$$

However, only one line of sight (1) is not sufficient to determine the position of the inspected floor where it intersects the vertical edge of the building wall (i.e. two equations fail to solve for three unknowns.) One more extra component as a constraint is required in order to define a third equation.

In seismic engineering, it is mainly the destructive forces of an earthquake coming along the horizontal direction that induce structural damage in buildings. The ATC-20 [1] is concerned with the rapid assessment of damage to buildings for entry and occupancy safety, and employs the tagging method to signal the state that a building is safe (green), unsafe (red) for use, or in restricted use (yellow). In practice, moderately damaged buildings, which only suffer from slight deformations, e.g., with the wall inclination of less than 3%, can still remain useful (tagged with green or yellow) as noted in [8]. Under such circumstances, the destructive forces usually do not cause torsion/twist deformation or foundation displacement of the buildings. As such, the inspected floors' deformation sustained by a damaged building in this research can be assumed to take place only on the walls whose axes are parallel or aligned to the shaking direction of the seismic forces (Fig. 5), due to which the deformed floors remain in a plane that is unchanged pre and post earthquake as shown in Fig. 5. The wall plane thus can serve as the extra component constraint for the line of sight, as modeled in (3):

$$AX_n + BY_n + C = 0 \tag{3}$$

Note that the wall plane is vertical to the ground such that the variable Z_n along Z-axis is not necessary for (3). The A, B, and C are the coefficients of the equation denoting the wall plane, which can be referred to from the pre-disaster outer geometry of the inspected building that is obtained or available a-priori from the building owners or government databases.

Using the line of sight formula (1) and the plane equation (3) where the wall deforms along the shaking direction, the coordinates (X_n, Y_n, Z_n) of the inspected floor along the building edge can be computed. Simply denoting (X_u, Y_u, Z_u) as the edge position of the inspected floor and (X_l, Y_l, Z_l) as that of the floor beneath, the interstory drift (ISD) of the inspected floor can be subsequently computed by (4), as follows:

$$\begin{aligned}
ISD &= (X_u - X_l)/|X_u - X_l| \\
&\quad \times \sqrt{(X_u - X_l)^2 + (Y_u - Y_l)^2}
\end{aligned} \tag{4}$$

where $(X_u - X_l)/|X_u - X_l|$ indicates direction of the inspected floor's movement, i.e. plus (+): along the X-axis, minus (−): against the X-axis, and $\sqrt{(X_u - X_l)^2 + (Y_u - Y_l)^2}$ calculates the absolute value of the movement.

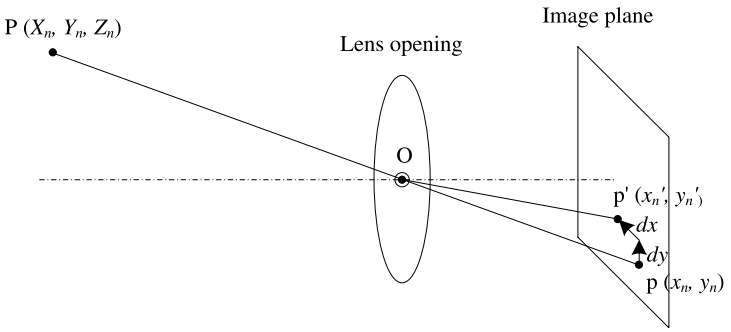

Fig. 6 Camera lens distortion inducing an offset between true and disturbed positions of a point on the image plane

Applying the photogrammetry assisted computing equations also needs the camera station' external components $(X_c, Y_c, Z_c, \alpha, t, s)$ and internal components (x_n, y_n, c) to be determined in advance so as to fit the parameters of the *collinearity equations* (1), which will be discussed in the following sections.

3 Measuring Camera Position and Orientation

The camera station's spatial coordinates (X_c, Y_c, Z_c) and orientation angles (α, t, s) are traditionally determined by means of identifying corresponding points on multiple images taken from different perspectives and fixing absolute position of camera by use of known reference points, giving rise to a lack of the ease of operation and applicability. In this research, we propose the Real Time Kinematics Global Positioning System (RTK-GPS) and a 3D electronic compass to measure the (X_c, Y_c, Z_c) and (α, t, s) of the camera's perspective respectively, which enables a maximum degree of freedom for the proposed method applied in the outdoor environment.

The RTK-GPS applied is the Trimble Ag GPS Base Station 900 with a horizontal accuracy of 1–2 ppm (parts-per-million) and vertical accuracy of 2–3 ppm (parts-per-million), namely, if the distance (baseline length) between the base station and the rover receiver is 10 km, the horizontal error of the RTK-GPS is 10–20 mm and its vertical error is 20–30 mm. Such technology has already been successfully used to monitor roof displacements in tall buildings [26, 27] and deformations in other types of large scale civil infrastructure [28, 29]. The 3D electronic compass is the PNI TCM 5 which uses the rotation definition of flight dynamics as per: $-90° \sim 90°$ in pitch, $-180° \sim 180°$ in roll, and $-180° \sim 180°$ in heading (yaw), and has a level of rotation accuracy of 0.3°. The mapping between the flight dynamics rotation angles and the photogrammetry tilted rotation angles for Earth Axes is as: azimuth (α) = heading, tilt $(t) = 90°+$ pitch, and swing $(s) = 180°-$ roll, if pitch $\leq 0°$; and azimuth $(\alpha) = 180°+$ heading, tilt $(t) = 90°+$ pitch, and swing $(s) = 180°-$ roll, if pitch $>0°$.

4 Evaluating Camera's Systematical Error

Camera systematical error refers to the measurement error on the image plane induced by the imperfection of the camera lens and its internal mechanics with a consistent effect that cannot be statistically eliminated [14]. In this section, we discuss two major aspects that induce the camera's systematical error, namely—the lens distortion and the approximation of the principal distance.

4.1 Lens Distortion

In an ideal situation, a spatial point P is projected through a camera lens opening (O) on the image plane to have an image point p, and the three points P, O, and p lie along a straight line (Fig. 6). But in reality owing to the lens distortion of the camera, the projected image point is shifted from its true $p(x_n, y_n)$ to a disturbed position p' (x_n', y_n') as illustrated in Fig. 6, resulting in an offset between the two positions. Denoting the offset by dx and dy, thus the true coordinates of any image point can be compensated by (5):

$$\begin{aligned} x_n &= x_n' + dx \\ y_n &= y_n' + dy \end{aligned} \tag{5}$$

For modern digital cameras, the camera lens distortion (i.e. dx and dy) can be taken as the aggregate of the radial distortion and the decentering distortion [15, 16]. As the lens of a camera is actually composed of a combination of lenses, the centers of those lens elements are not strictly collinear, giving rise to the decentering distortion. In contrast, the radial distortion occurs in each single optical lens and the distortion effect is magnified along the radial direction of the lens: the further a point is away from the center of the lens, the larger error is produced for its projected image point. Therefore, dx, dy can be decomposed by (6):

$$\begin{aligned} dx &= dx_r + dx_d \\ dy &= dy_r + dy_d \end{aligned} \tag{6}$$

in which dx_r, dy_r is the radial distortion along x-axis, and y-axis; and dx_d, dy_d is the decentering distortion along x-axis, and y-axis. Assuming the optical axis of the lens is

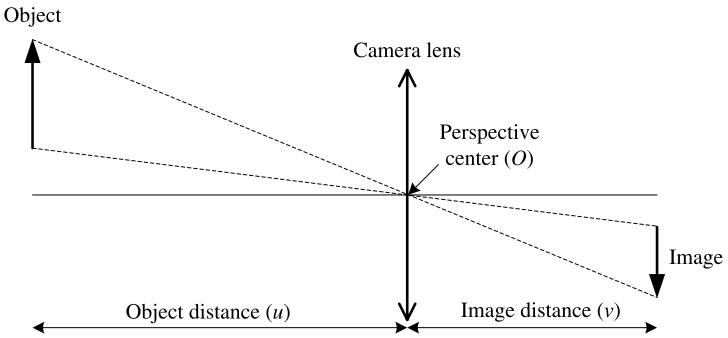

Fig. 7 Illustrated object distance and image distance when a camera is photographing an object

perpendicular to the image plane, Brown [17] developed the mathematical model for correcting the lens distortion by (7):

$$
\begin{aligned}
dx_r &= K_1(x'_n - x_p)r^2 + K_2(x'_n - x_p)r^4 + K_3(x'_n - x_p)r^6 \\
dy_r &= K_1(y'_n - y_p)r^2 + K_2(y'_n - y_p)r^4 + K_3(y'_n - y_p)r^6 \\
dx_d &= P_1[r^2 + 2(x'_n - x_p)^2] + 2P_2(x'_n - x_p)(y'_n - y_p) \\
dy_d &= P_2[r^2 + 2(y'_n - y_p)^2] + 2P_1(x'_n - x_p)(y'_n - y_p) \\
r^2 &= (x'_n - x_p)^2 + (y'_n - y_p)^2
\end{aligned}
\tag{7}
$$

Here x_p and y_p are the coordinates of the principal point, K_1, K_2 and K_3 are the radial distortion parameters, and P_1 and P_2 are the decentering distortion parameters. A camera calibration can be used to determine the lens distortion parameters.

4.2 Approximated Principal Distance

The *principal distance* (c) of a camera in photogrammetry is defined as the distance of the perpendicular line from the *perspective center* (center of lens opening) to the image plane of the camera, which is approximated as the *focal length* (f) of the camera in the *collinearity equations* of (1). In this research, we seek the actual principal distance instead of the approximated camera focal length as the reconnaissance task requires the achievable level of measurement accuracy to be as high as possible.

Figure 7 shows a camera photographing an object where the photographic object distance and the image distance are illustrated. The principal distance c equals the image distance v when the image plane is at the exact position along the optical axis that an object is clearly focused. Meanwhile, the distance between the object and the camera lens is defined as object distance u. The conjugated distances u, v and the focal length f are related by the *lens conjugate equation* [18] as: $1/u + 1/v = 1/f$, by which the image distance can be derived by (8):

$$
v = \frac{uf}{u - f} \tag{8}
$$

Equation (8) computes the actual length of the principal distance. Also, as an object is actually shot, the object distance u usually is much farther than the image distance v. As such, the denominator $(u - f)$ can be approximated as u, which yields: $v \approx f$. This proves the assertion that the *principal distance* (c) can be practically approximated to the focal length of the camera lens when focused at infinity, namely, $c \approx f$.

5 Camera Calibration

5.1 Description of Calibration

The calibration procedure is important for the successful implementation of this post-earthquake reconnaissance method, and its goal is to determine the camera's lens distortion parameters and interior parameters in terms of the fine-tuned focal length and the displacement of the principal point in a single run. The camera calibration usually involves two steps: (1) taking the calibration photos, and (2) deriving the camera parameters with those photos. This research utilized a camera calibrator in the well-established commercial software system—PhotoModeler® [19] to perform the calibration, which prevails both in the industrial market and in the research field.

Twelve photos of a calibration grid are recommended to be taken from four edges of the grid with a combination of a portrait orientation and two landscape orientations (left and right) [20]. The camera's focal length needs to be kept constant during the entire course of photo taking. In order to ensure that the entire lens is calibrated, the photo frames should cover as much as possible the grid dots when taking photos, and each four photos should have the grid dots aligned along the left, right, and top and bottom edge of the photo respectively (as illustrated in Fig. 8a). The calibration grid is a pattern of dots designed specifically for the camera calibrator in PhotoModeler®, and the camera calibrator is a computer program running the algorithm to automate the derivation of camera parameters. Figure 8b shows the cameras' positions and orientations when twelve photographs were exposed in PhotoModeler® as part of the camera calibration result.

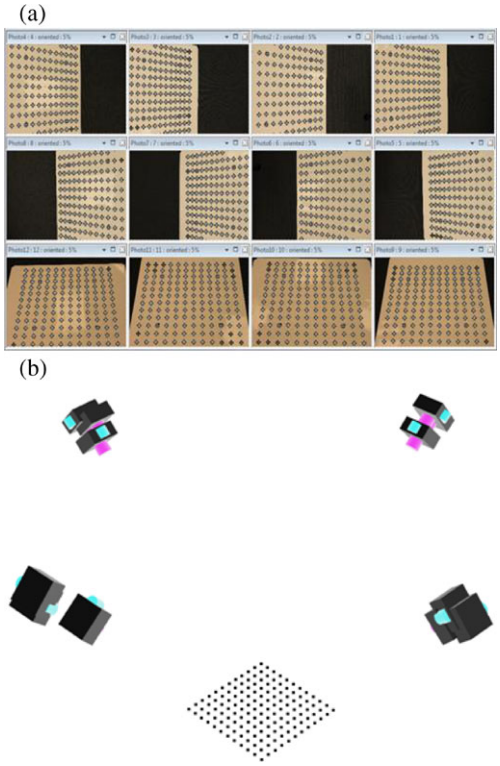

Fig. 8 Illustrated (**a**) calibration grid dots covered in twelve photos, and (**b**) twelve camera positions evaluated in PhotoModeler® as part of camera calibration result

5.2 Calibration Results

The camera used to imitate the inspector's camera in this research was an off-the-shelf digital single lens reflection (DSLR) camera—Canon EOS REBEL T1i with its focal length set at 55 mm to obtain the longest shooting range of the camera. By following the calibration procedure described above, we obtained the calibration results for the designated camera as: the radial lens distortion parameters ($K_1 = -2.203\text{e–}005$, $K_2 = -1.267\text{e–}008$, $K_3 = 0$), decentering lens distortion parameters ($P_1 = -1.179\text{e–}004$, $P_2 = 0$), the image coordinates (x_p, y_p) of the principal point (12.1573 mm, 7.7877 mm), and the adjusted focal length ($f = 55.4121$ mm). The threshold for evaluating the quality of calibration is that the maximum residuals are less than one pixel [20]. In this research, this calibration yielded the maximum residuals value as 0.9191, reflecting a good calibration of the camera parameters. A residual here means the discrepancy of the distance between the calibrated each grid dot and its most likely value that is statistically calculated.

It is noteworthy that the calibration work is only needed during the first time of using the camera to take source photos. As long as the focal length doesn't change, successive modeling work can use the same calibration results to determine the internal camera parameters. The obtained camera interior parameters and lens distortion parameters will be used to calculate the undistorted coordinates of the projected image points in the experiments in order to test the validity of the proposed method, which is discussed in the next section.

6 Laboratory Experiments and Results

The indoor experiments were conducted in the UM Construction Laboratory to validate the feasibility of the proposed earthquake reconnaissance method. In the first phase, we primarily focused on the internal components of a digital camera that account for the measurement error. Thus, we used physical measurements rather than the RTK-GPS to manually measure the 3D coordinates of the camera position. Figure 9a gives an overview of the setup for the experiment environment, in which a two storey reconfigurable steel frame was installed to mimic a building structure.

The frame was calibrated with known precise displacement values at the second floor. To measure the camera's rotation angles, a 3D electronic compass was customized with a flat plate attached on the camera's hot shoe, and the angle readings were transmitted real time to a connected laptop with a data wire (Fig. 9b). The interstory drift between the second and third floor of the frame was studied in this experiment, and the positions of the inspected floors were denoted by two bolted connections that lie along the left edge of the frame as illustrated in Fig. 9c. Subtracting the horizontal axis components of the two connections thus helped compute the desired interstory drift.

The parameters for line of sight of the camera (*collinearity equations* (1)) were fitted with the measured camera's coordinates and angles together with the adjusted camera focal length. For ease of computation, we simply assume that the X-axis of the global coordinate system is aligned with the horizontal movement of the inspected floors, the Z-axis is perpendicular to the ground that points upward, and the origin is at the left frontal corner of the frame (Fig. 9a). As such, the formula of plane to represent the inspected wall was obtained as $Y = 0$. Using the derived *collinearity equations* and the formula of the wall plane, the spatial coordinates of horizontal axes for the bolted connections could be calculated from the captured images. Subsequently, the interstory drift could be determined.

The camera setup was as follows: the position fixed at the coordinates (−0.489, 5.613, 1.34) m with the focal length set at 55 mm. Three groups of experiments were conducted, where each group had the camera's perspective rotated about the horizontal angle (azimuth) within a certain range to extensively verify the complementarities and adaptability of the proposed method to augmented reality visualization. In the experiment, the line of sight of the camera was intentionally arranged not perpendicular to the frontal wall of

Table 1 Second-story drifts measured using photogrammetry

Frame No.	Group 1		Group 2		Group 3	
	Drift (mm)	Error (mm)	Drift (mm)	Error (mm)	Drift (mm)	Error (mm)
1	−50.81	−5.81	−47.61	−2.61	−51.26	−6.26
2	−51.02	−6.02	−46.97	−1.97	−51.28	−6.28
3	−50.16	−5.16	−46.66	−1.66	−50.73	−5.73
4	−51.08	−6.08	−47.18	−2.18	−50.75	−5.75
5	−51.18	−6.18	−47.48	−2.48	−51.16	−6.16
6	−51.33	−6.33	−47.34	−2.34	−51.41	−6.41
7	−50.55	−5.55	−47.64	−2.64	−51.11	−6.11
8	−50.35	−5.35	−47.17	−2.17	−51.23	−6.23
9	−51.16	−6.16	−46.79	−1.79	−51.61	−6.61
10	−51.10	−6.10	−47.17	−2.17	−51.58	−6.58
Average Error (mm)		−5.87		−2.20		−6.21
Error Std Dev (mm)		0.39		0.33		0.30

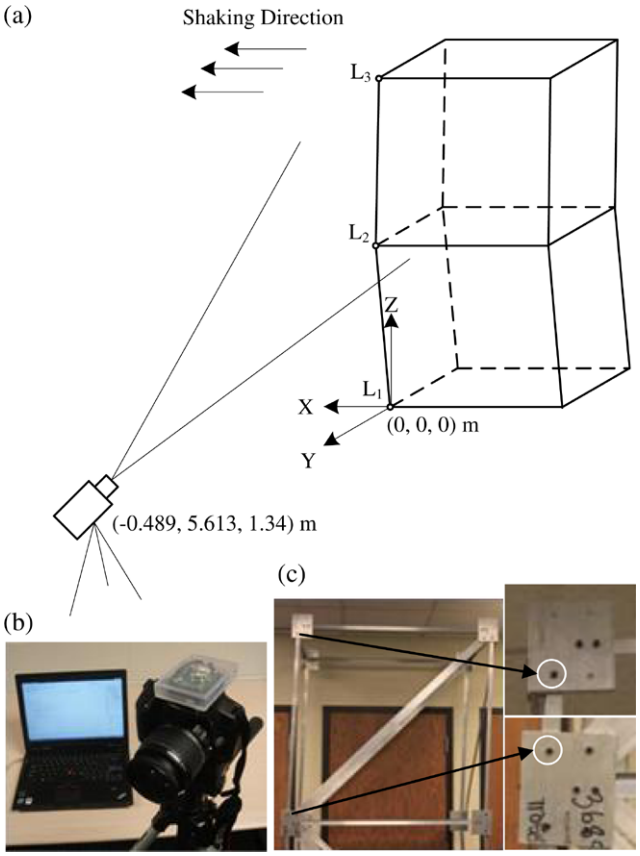

Fig. 9 (**a**) Experiment setup overview, (**b**) customized compass attached on the camera, and (**c**) bolted connections denoting positions of two inspected floors

the frame and had a variation with respect to the horizontal plane as per 8.15°, 4.29°, and 7.44° in average for each group. Figure 10 shows three selected photos of the second and third floors to the frame that were exposed from aforementioned horizontal perspectives in three experiments. The calibrated actual displacement was 45 mm to the left. The resulting measurements of the three experiments are presented in Table 1.

The implemented algorithm is running on a commonly used laptop computer—Lenovo ThinkPad SL400 (Intel Core 2 Duo CPU T5670 @1.8 GHz, and RAM 2.0 GB) that is deployable with the reconnaissance system readily to be equipped in the inspector's backpack. For this two-story structure, the computation took less than one second for each measured drift. It must also be noted that for any given actual building, the number of points at which the drift must be computed is relatively finite, making the proposed approach well suited for rapid measurement on several buildings in a short amount of time.

The average errors for three groups of drift measurements are −5.87, −2.2, and −6.21 mm respectively with small standard deviations (Group 1: 0.39 mm, Group 2: 0.33 mm, Group 3: 0.3 mm), all indicating an acceptable and useful level of accuracy of the proposed method with statistical reliability. In addition, the best observation (i.e. average error) of drift measured by the proposed method occurred in Group 2, i.e. −2.2 mm, where the optical axis of the camera had the smallest angle (i.e. 4.29°) with the perpendicular line of the frame's wall plane. Thus, it can be concluded that the interplay of position and orientation measurements leads to the differences in average error obtained from set to set: the closer the camera orthogonally shoots a damaged structure, the better the measured accuracy of the proposed method will be. Group 1 and Group 3 had similar orders of accuracy that were obtained from similar horizontal angles set, thereby quantitatively proving the consistency of the method.

The experimental results also reveal that the photos taken under the indoor laboratory condition (illuminated by fluorescent lamp) can have a satisfactory quality for apply-

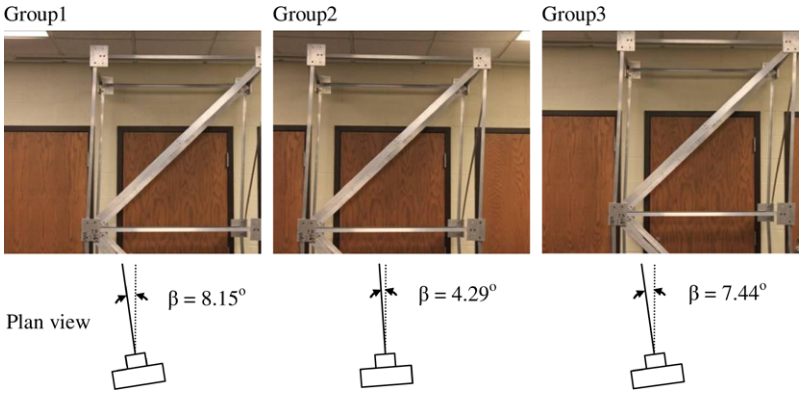

Fig. 10 Selected photos of the second and third floors of the frame in three experiments that were exposed from different horizontal angles (β = variation angle to horizontal orthogonal line)

ing photogrammetry. The camera used was an off-the-shelf Canon EOS REBEL T1i with the maximum resolution 15 mega pixels and autofocus functionality, which lends itself well to adjustments and calibration based on environmental conditions prevalent at the time. Therefore, it is expected that photos with even higher quality would be taken in an outdoor setting, where the reconnaissance method will be eventually deployed. Additionally, the other devices that have been used in the prototype (GPS and compass) have also shown no observable discrepancy in varying outdoor conditions in the authors' experiments.

Unlike monitoring the structure alignment during operations such as tunneling, currently there are no specific criteria that indicate tolerances for a method used in seismic damaged building drift measurement. However, to the authors' best knowledge and understanding, based on the typical height of building floors, uncertainty (or error) of approximately 5 mm in the measurement of drift is not of significance in terms of drift interpretation and is therefore of acceptable accuracy or usefulness for the intended purpose.

7 Conclusions and Future Work

This paper proposed a semi-automated method to rapidly measure structural damage induced in tall buildings by seismic events such as earthquakes or explosions by applying close-range photogrammetry surveying techniques and Augmented Reality (AR) visualization. Analytical measurement algorithms were devised, lens distortion and approximated calculation of camera focal length that account for camera systematical error were assessed, and laboratory experiments were conducted to validate measurement accuracy. It should be noted that this research proposes an approximate yet applicable approach to rapidly measure the damage in buildings sustained during a seismic disaster, and the readily deployable consumer grade equipment that has been employed in evaluating our approach has distinct advantages in this application over commercial high-end photogrammetry equipment that can offer higher measurement accuracy but can also be prohibitively expensive, requires higher setup times, and can be challenging from a mobility perspective.

It is worth mentioning that in another study, the authors used a lower resolution 10 megapixel Canon Eos 400D camera to conduct measurements of building products, yielding an accuracy level of 10 mm [21]. In this research, the camera used was the newly released Canon EOS REBEL T1i with a maximum resolution of 15 megapixels. The two models of cameras have similar prices, but with the newer model, a 5 mm level of accuracy was achieved, revealing that applying a camera with higher resolution can substantially increase the accuracy of the photogrammetric measurement. It can be foreseen that more accurate measurement results can be obtained by the proposed method as the advances in optical-sensing technology and camera manufacturing progress.

Future extension of the presented research is to implement the proposed reconnaissance method in non-laboratory outdoor conditions that real life seismic disasters occur in. External tracking Global Positioning Systems will be integrated to account for overall accuracy of this technique in extrapolating the interstory drifts. Recent advances in satellite transmission technology allow the dual-frequency GPS receivers to achieve a centimeter level of accuracy for RTK measurements without a base station (Trimble® Vrs Now™) [22], which promises to overcome the technical hurdle of tracking the inspector's (camera's) perspective for the proposed technique to be deployed in the field.

In order to address situations where GPS positioning might be challenging due to the urban canyon problem, the research team is also working on a hybrid localization approach where emergency response vehicles with optimum visibility to GPS satellites can position themselves at specific urban locations, and then serve as terrestrial base stations, relative to which the mobile inspectors can be localized using a terrestrial or line-of-sight based technology. The electronic compass used in our study also has several different options available. The devices used in the current prototype, and their inherent measurement uncertainties (or

errors) propagate in the uncertainty in the measured drift. Future prototypes or implementations could use alternate, more accurate methods for obtaining position and orientation which would translate in further improving the accuracy of the measured drift.

Another extension is an endeavor toward full automation of the reconnaissance method by looking into techniques in the research area of computer vision for direct detection of edges of key floors sustained in a damaged building on images. Preliminary study by the authors has found that the outline of a damaged building can be effectively extracted by the Active Contours technique [23] embedded in Augmented Reality visualization. Nonetheless, the technique's validity and applicability needs to be further meticulously investigated.

Acknowledgements This presented research was partially funded by the US National Science Foundation (NSF) under Grant CMMI-0726493. The writers gratefully acknowledge NSF's support. This research was also partially supported by the PhD student overseas exchange program of the Hong Kong Polytechnic University (PolyU). Any opinions, findings, conclusions, and recommendations expressed in this paper are those of the authors and do not necessarily reflect the views of the NSF or PolyU.

References

1. Applied Technology Council (ATC): Procedures for postearthquake safety evaluations of buildings. Rep. No. ATC-20, Redwood City, CA (1989)
2. Applied Technology Council (ATC): Addendum to ATC-20: procedures for postearthquake safety evaluations of buildings. Rep. No. ATC-20-2, Redwood City, CA (1995)
3. Kamat, V.R., El-Tawil, S.: Evaluation of augmented reality for rapid assessment of earthquake-induced building damage. J. Comput. Civ. Eng. **21**(5), 303–310 (2007)
4. Rathje, E., Crawford, M.: Using high resolution satellite imagery to detect damage from the 2003 northern Algeria earthquake. In: 13th World Conference on Earthquake Engineering, August 1–6, Vancouver, BC, Canada (2004). Paper No. 2911
5. Turker, M., Sumer, E.: Building-based damage detection due to earthquake using the watershed segmentation of the post-event aerial images. Int. J. Remote Sens. **29**(11), 3073–3089 (2008)
6. ScienceDaily: World's highest-resolution commercial satellite. Available via http://www.sciencedaily.com/releases/2009/05/090526183858.htm. Accessed 23 August 2010
7. Skolnik, D.A., Wallace, J.W.: Critical assessment of interstory drift measurements. J. Struct. Eng. **136**(12), 1574–1584 (2010)
8. Los Angeles Tall Building Structural Design Council (LATBSDC): An alternative procedure for seismic analysis and design of tall buildings located in the Los Angeles Region, Los Angeles (2008)
9. Blachut, T.J., Burkhardt, R.: Historical development of photogrammetric methods and instruments. In: ASPRS, Falls Church, VA, pp. 4–18 (1989). Chap. 1
10. Federal Emergency Management Agency (FEMA): Recommended seismic design criteria for new steel moment-frame buildings. Rep. No. 350, Building Seismic Safety Council, Washington, DC (2000)
11. Wong, K.W.: Basic mathematics of photogrammetry. In: Slama, C.C. (ed.) Manual of Photogrammetry, ASPRS, Falls Church, VA, pp. 37–101 (1980). Chap. 2, 4th edition
12. Wolf, P.: Elements of Photogrammetry. McGraw-Hill, New York (1983)
13. McGlone, J.C.: Analytic data-reduction schemes in non-topographic photogrammetry. In: Karara, H.M. (ed.) Non-topographic Photogrammetry, ASPRS, Falls Church, VA, pp. 37–55 (1989). Chap. 4, 2nd edition
14. Viswanathan, M.: Measurement Error and Research Design. Sage Publications, Thousand Oaks (2005)
15. Beyer, H.A., Uffenkamp, V., van der Vlugt, G.: Quality control in industry with digital photogrammetry. In: Gruen, A., Kahmen, H. (eds.) Optical 3-D Measurement Techniques III, pp. 29–38. Wichmann, Heidelberg (1995)
16. Fraser, C.S.: Industrial measurement applications. In: Atkinson, K.B. (ed.) Close Range Photogrammetry and Machine Vision, Whittles, Scotland, pp. 329–361 (1996). Chap. 12
17. Brown, D.C.: Decentering distortion of lenses. Photogramm. Eng. **32**(3), 444–462 (1966)
18. Ray, F.S.: Photographic optics. In: Morton, A.R. (ed.) Photography for the Scientist, 4th edn., pp. 104–124. Academic Press, Orlando (1984). Chap. 2
19. Eos Systems Inc.: PhotoModeler: close-range photogrammetric measurement and 3D modeling software. Available via http://www.photomodeler.com (2009). Accessed 20 October 2009
20. Eos Systems: User Manual for PhotoModeler® Pro Version 5, Vancouver, BC (2004)
21. Dai, F., Lu, M.: Assessing the accuracy of applying photogrammetry to take geometric measurements on building products. J. Constr. Eng. Manag. **136**(2), 242–250 (2010)
22. Trimble Navigation Limited: Trimble® Vrs Now™: a real RTK network solution for GPS rover to receive high quality, location independent correction data. Available via http://www.trimble.com/vrsnow.shtml (2010). Accessed 31 July 2010
23. Caselles, V., Kimmel, R., Sapiro, G.: Geodesic active contours. Int. J. Comput. Vis. **22**(1), 61–79 (1997)
24. Imaging Mesa: SR4000 camera overview. Available via http://www.mesa-imaging.ch/prodview4k.php (2011). Accessed 21 May 2011
25. PMDTechnologies GmbH: CamCube 3.0 camera overview. Available via http://www.pmdtec.com/products-services/pmdvisionr-cameras/pmdvisionr-camcube-30 (2011). Accessed 21 May 2011
26. Celebi, M., Sanli, A.: GPS in pioneering dynamic monitoring of long-period structures. Earthq. Spectra **18**(1), 47–61 (2002)
27. Tamura, Y., Matsui, M., Pagnini, L.C., Ishibashi, R., Yoshida, A.: Measurement of wind-induced response of buildings using RTK-GPS. J. Wind Eng. Ind. Aerodyn. **90**(15), 1783–1793 (2002)
28. Nakamura, S.: GPS measurement of wind-induced suspension bridge girder displacements. J. Struct. Eng. **126**(12), 1413–1419 (2000)
29. Hudnut, K.W., Behr, J.: A continuous GPS monitoring of structural deformation at Pacoima Dam, CA. Seismol. Res. Lett. **69**(4), 299–308 (1998)